Carbohydrate Polymers 83 (2011) 1253–1256

Contents lists available at ScienceDirect

Carbohydrate Polymers

journal homepage: www.elsevier.com/locate/carbpol

Regenerated bacterial cellulose fibers prepared by the NMMO·H_2O process

Qiuying Gao, Xinyuan Shen*, Xinkun Lu

State Key Laboratory for Modification of Chemical Fibers and Polymer Materials, College of Material Science and Engineering, Donghua University, Shanghai 201620, People's Republic of China

ARTICLE INFO

Article history:
Received 19 July 2010
Received in revised form 2 September 2010
Accepted 16 September 2010
Available online 15 October 2010

Keywords:
Bacterial cellulose
Regenerated fibers
N-methylmorpholine-N-oxide monohydrate (NMMO·H_2O)
Wet spin

ABSTRACT

In this work, bacterial cellulose (BC) was dissolved in N-methylmorpholine-N-oxide monohydrate (NMMO·H_2O), and regenerated BC fibers were prepared. Structure and properties of the regenerated BC fibers were characterized by different techniques such as scanning electron microscopy (SEM), fourier transform infrared spectroscopy (FTIR), x-ray diffraction (XRD), thermogravimetric analysis (TGA), and single filament electric tenacity tester. Results revealed that whole fibers showed a circular shape with fairly regular size along the fiber axis. There was no significant difference between the structure of native BC and the regenerated BC fibers. The regenerated BC fibers had a cellulose II crystalline structure, lower degree of crystallinity, smaller crystallite sizes, and better thermal stability than the native BC. Tensile strength of the regenerated BC fibers was 0.5–1.5 cN/dtex, and their extension at break was 3–8%.

1. Introduction

Bacterial cellulose (BC) is a kind of biosynthetic polymer, which is a kind of specific product of primary metabolism and synthesized by bacteria such as Acetobacter, Rhizobium, Agrobacterium, and Sarcina (Jonas & Farah, 1998). Its most efficient producers are acetic acid bacteria Acetobacter xylinum (Brown, 1886; Ross, Mayer, & Benziman, 1991). As opposed to plant cellulose (PC), BC does not require remedial process to remove unwanted polymers and contaminants, therefore retains a greater degree of polymerization. In a native state, BC has many excellent properties, such as high purity, high degree of polymerization (DP), crystallinity, hydrophilicity and biocompatibility, etc. Because of its unique properties resulting from the ultrafine reticulated structure, BC has a multitude of applications in different fields, including composite membranes, medicine, artificial skins, blood vessels, and binding agents (Pommet et al., 2008; Svensson et al., 2005).

N-methylmorpholine-N-oxide (NMMO) is usually used as a solvent for direct dissolution of cellulose in industrial fiber-making (e.g. Lyocell process) (Fink, Weigel, Purz, & Ganster, 2001; Lock, 1992). The process is environmentally protective because the NMMO is nontoxic and can be almost completely recycled with more than 99% recovery proportion (Rosenau, Potthast, Sixta, & Kosma, 2001). The hydration number of NMMO hydrates has a significant effect on the solution's solubility. N-methylmorpholine-N-oxide monohydrate (NMMO·H_2O) could fully dissolve cellulose which produce a solution with good spinnability. In this article, the NMMO·H_2O was used as the solvent of BC, the BC/NMMO·H_2O solution was then used to spin the regenerated BC fibers, and the structure and properties of the regenerated BC fibers were compared with those of native BC.

2. Materials and methods

2.1. Materials

Bacterial cellulose powder was bought from shengfengdengtai Biotechnology Co., Ltd. (Jiang Su, China). Its degree of polymerization (DP) was about 2700. N-methyl-morpholine-N-oxide (NMMO) powder, obtained from commercial sources, was mixed with a certain amount of H_2O to be NMMO·H_2O. Propyl gallate (PG), obtained from commercial sources too, was used as an antioxidant to avoid oxidation and degradation during the bacterial cellulose dissolving (Rosenau et al., 2002).

2.2. Dope preparation

To obtain NMMO·H_2O solution, an adequate amount of H_2O was added to NMMO power (the value of H_2O was about 13.3%, w/w). The mixture was heated at 90 °C for 30 min. After that, BC powder was added into that NMMO·H_2O solution (the BC concentration was 7 wt% in the obtained BC/NMMO·H_2O solution). In order to prepare a homogeneous solution, the dispersions were heated at 80 °C for 12 h, with a fast energetic stirring. Air bubbles were trapped in the

* Corresponding author. Tel.: +86 21 67792870; fax: +86 21 67792855.
E-mail address: shenxy@dhu.edu.cn (X. Shen).

0144-8617/$ – see front matter.
doi:10.1016/j.carbpol.2010.09.029

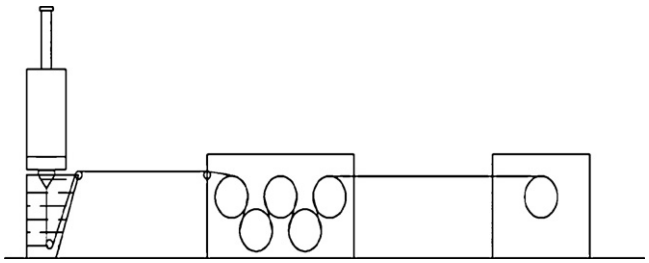

Fig. 1. Schematic representation of the wet spinning line.

solutions, due to the fast energetic stirring. So before spinning, the centrifugation of the dopes at high temperature was used in order to disengage air bubbles. After the centrifugation step, no phase separation was observed.

2.3. Spinning

Fig. 1 shows the wet spinning line used to produce the regenerated BC fibers. This wet spinning line is composed of an extrusion unit with varied extrusion rate and spinneret diameter, a coagulation bath and two sets of spools, thread take-up and roller. The collecting rate of the spinning line can be varied so that fibers are collected with different drawn ratios, defined as the ratio between spools' speed and fiber velocity at the spinneret hole, or rather when no stretch is applied during coagulation. There are 30 holes in the spinneret, and the diameter of these holes is 0.08 mm. About 500 g fibers can be prepared in 24 h. In this article, the extrusion rate was 14.67 m/min, BC solutions were spun at 80 °C and coagulated in deionized water at 0 °C, and then collected fibers were washed in deionized water for about 48 h in order to extract residual NMMO and dried under vacuum at 50 °C for 24 h. At last, the fibers were stored over silica gel until testing.

2.4. Microscopic analysis

Scanning electron microscopy (SEM) was used to observe sample morphology and microstructure. Samples were sputter coated with gold and examined using a JEOL JSM-5600LV microscope (Japan).

2.5. Fourier transform infrared spectroscopy (FTIR) analysis

The surface properties of the samples were tested using a fourier transform infrared spectrometer (FT-IR NEXUS-670, USA). The FT-IR spectra were recorded in a spectral range of 400–4000 cm^{-1} at a resolution of 4 cm^{-1}, and the scan speed was 0.2 cm/s. The samples were mixed with potassium bromide (KBr) and pressed into pellets. The background spectrum was subtracted from the sample spectra.

2.6. X-ray diffraction (XRD) analysis

The crystalline structure of the samples was examined using a wide angle x-ray diffractometer (D/max-2550 PC, Japan) .The samples were scanned from $2\theta = 0$–60°, the operating voltage and current were 40 kV and 200 mA, respectively. The radiation was Ni-filtered Cu-Ka radiation of wavelength 1.54056 Å.

The degree of crystallinity (X_c) was calculated by the ratio of the area in a diffractogram corresponding to the crystalline region to that of both crystalline (S_c) and amorphous regions (S_a) (Dwianto et al., 1998):

$$X_c = \frac{S_c}{(S_c + S_a)} \quad (1)$$

The crystal sizes of the cellulose samples were calculated by Scherrer equation:

$$L_{(hkl)} = \frac{K\lambda}{\beta \cos\theta} \quad (2)$$

where λ is the wavelength of the employed x-ray radiation, 1.54056 Å, $K = 0.9$, β is the full width half maximum, in radian, and θ is the diffraction angle (Hindeleh & Johnson, 1972; Zhu, Zhang, Hong, & Yin, 2005).

2.7. Thermal analysis

Thermogravimetric analysis (TGA) measurements on samples were performed with a TGA instrument (TGA 309F1, USA), from room temperature to 700 °C, at a heating rate of 10 °C/min, on 2–5 mg samples. The open Al_2O_3 cell was swept with N_2 during the whole analysis.

2.8. Mechanical properties

Mechanical properties of single fibers were measured using XQ-1 single filament electric tenacity tester (China), with a 20 mm gauge length at a crossbar rate of 30 mm/min. The tenacity and extension at break of the regenerated BC fibers were calculated as the average of at least 30 measurements.

3. Results and discussion

3.1. SEM morphology

Fig. 2 shows the scanning electron microscope (SEM) photographs of the native BC and the regenerated BC fibers. Picture (a) was the SEM photo of the native BC which was powdered. Picture (b) indicated the surface of the regenerated BC fibers. The whole fibers showed a circular shape with fairly regular size along the fiber axis. However, the surface of the fibers was not smooth, there were some longitudinal striations. Those striations were beneficial to later dyeing. Picture (c) showed the cross-sections of the regenerated BC fibers. The regenerated BC fibers showed a compact structure, even though there were a few voids in the cross-sections.

3.2. FT-IR data

Fig. 3 shows the FT-IR spectra of the native BC and the regenerated BC fibers. In these data, the –OH stretching peak was 3416 cm^{-1}, and the $-CH_2$ stretching peak 2921 cm^{-1}. The band at 1644 cm^{-1} was due to the stretching of H–O–H (Belousova, Shablygin, Belousova, Golova, & Papkov, 1986), which was adsorbed on the surface of BC. The absorption bands present in both native BC and regenerated BC fibers were 1375 cm^{-1}, 1160 cm^{-1} and 1065 cm^{-1}, which can be attributed to C–H scissor vibration (Belousova et al., 1986), –OH wagging vibration (Liang & Marchessault, 1959), and C–O and C–C stretching vibration respectively (Smidt, Lechner, Schwanninger, Haberhauer, & Gerzabek, 2002). From the figure we can see both the native BC and the regenerated BC fibers shows a similar FT-IR spectra, which means there was no significant difference between the structure of the native BC and regenerated BC fibers. There were only some physical changes during the whole dissolving and spinning process.

3.3. X-ray data

With most synthetic and natural polymeric fibers, their mechanical properties were largely affected by various structural parameters such as crystallinity and molecular orientation. In order to determine the structural parameters of the fibers, the XRD

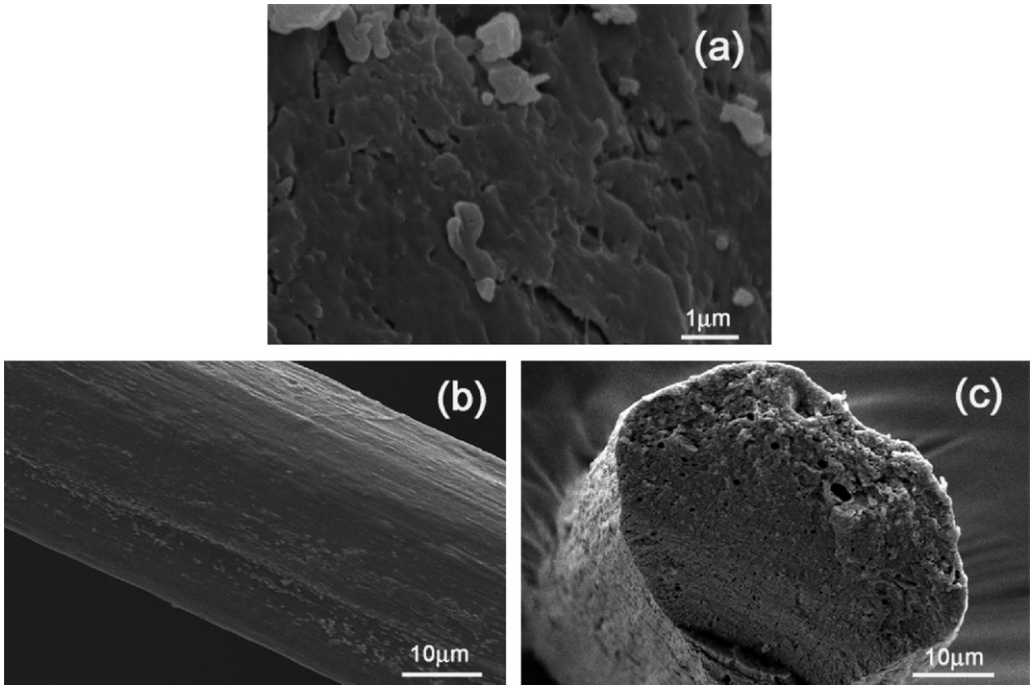

Fig. 2. SEM photographs of the native BC and the regenerated BC fibers.

measurements were conducted. The results showed that the regeneration of BC resulted in significant changes in crystalline structure, crystallinity, and degree of orientation. In curve a (Fig. 4), native BC showed three strong Bragg peaks at about $2\theta = 14.4^\circ$, 16.7° and 22.6° which were indexed as the (1 0 1), (1 0 $\bar{1}$) and (0 0 2) peaks of the typical cellulose I structure respectively. In the XRD curve of the regenerated BC fibers (Fig. 4b), we also found three strong Bragg peaks at about $2\theta = 11.9^\circ$, 20.2° and 21.9° which were indexed as the (1 $\bar{1}$ 0), (1 1 0) and (2 0 0) peaks of the cellulose II crystal structure respectively (Zhang et al., 2010). These results indicated that the transformation from cellulose I to cellulose II occurred after the dissolution and spinning.

The degree of crystallinity and the crystallite sizes calculated from XRD data using Eqs. (1) and (2) were listed in Table 1. They clearly demonstrate that the degree of crystallinity of native BC was 74.14%, but the degree of crystallinity of the regenerated BC fibers was 60.83%. The crystallite sizes of the regenerated BC fibers were smaller than the native BC. Since the growing of crystallites after regeneration was incomplete.

Table 1
Degree of crystallinity and the crystallite sizes of native BC and the regenerated BC fibers.

Sample	X_c (%)	L (*hkl*) (Å)	
		(101) (1 0 $\bar{1}$) (002)	(1 $\bar{1}$ 0) (110) (200)
Native BC	74.14	80 120 81	– – –
Regenerated BC fibers	60.83	– – –	26 30 54

3.4. TGA data

Thermal behaviors of the samples were investigated by TGA from 30 °C to 600 °C at 10 °C/min (Fig. 5). The curve of the native BC (Fig. 5a) showed that the weight loss due to the evaporation of

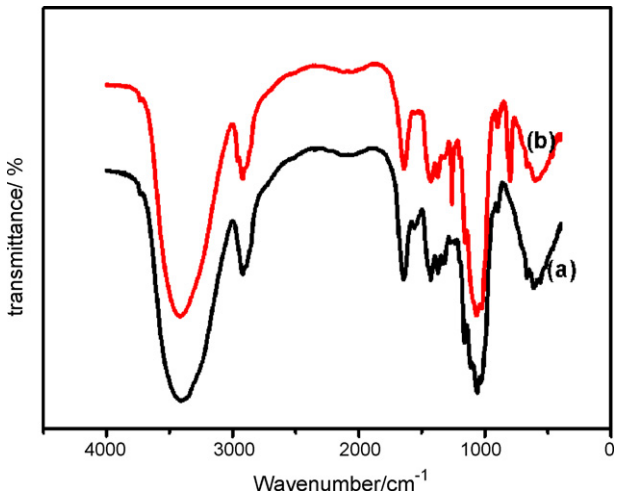

Fig. 3. FT-IR spectra of the native BC (a) and the regenerated BC fibers (b).

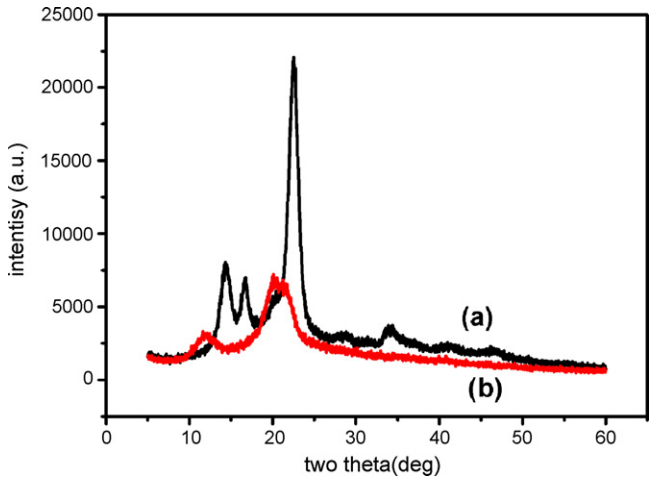

Fig. 4. X-ray diffraction curves of the native BC (a) and the regenerated BC fibers (b).

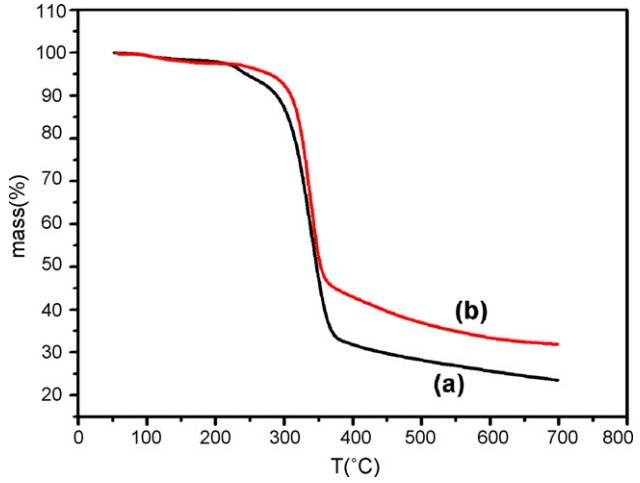

Fig. 5. TGA curves of the native BC (a) and the regenerated BC fibers (b).

Table 2
Tenacity and extension at break of some kinds of fibers.

	Tenacity (cN/dtex)	Extension at break (%)
Regenerated BC fibers	0.5–1.5	3–8
Cuprammonium rayon	1.5–2.0	7–23
Viscose rayon	2.0–2.4	20–25
Lyocell fiber	4.0–4.4	14–16

the H_2O adsorbed on the surface of BC cellulose mostly occurred up to about 85 °C. From 85 °C to 310 °C, the mass almost unchanged. Further weight loss from 310 °C to 365 °C was relatively fast, which was due to dehydration and decomposition of the molecules. The mass decreased about 66.69%. At last, from 365 °C to 700 °C, the mass decrease was less from the curve. However, the curve of the regenerated BC fibers (Fig. 5b) illustrated that the dehydration and decomposition of the molecules began at 320 °C, and the residual mass of curve (b) was more than curve (a). All of above showed that the thermal stability of the regenerated BC fibers was better than the native BC.

3.5. Mechanical properties of regenerated cellulose fibers

The mechanical properties of the regenerated BC fibers studied were presented in Table 2. It was noted that the regenerated BC fibers possessed relatively low tensile strength (0.5–1.5 cN/dtex), closed to Cuprammonium rayon (1.5–2.0 cN/dtex). The tenacity of the commercial viscose rayon (2.0–2.4 cN/dtex) (Liu, Shao, & Hu, 2001) and Lyocell fiber (4.0–4.4 cN/dtex) (Liu, Shen, Shao, Wu, & Hu, 2001) were higher than the regenerated BC fibers. So more research should be made to improve the mechanical properties of the regenerated BC fibers.

4. Conclusion

This study shows the possibility to obtain regenerated BC fibers, by using a wet spinning line, starting from BC/NMMO·H_2O solutions. The microscopic analysis, thermal analysis, FTIR analysis, XRD analysis, and mechanical properties of the native BC powder and regenerated BC fibers were investigated. It was demonstrated that there were some longitudinal striations on surface of the fibers. There was no significant difference between the structure of the native BC and the regenerated BC fibers. The regenerated BC fibers had a cellulose II crystalline structure, lower degree of crystallinity, smaller crystallite sizes, and better thermal stability than the native BC. Moreover, tensile strength of the regenerated BC fibers was 0.5–1.5 cN/dtex, and their extension at break was 3–8%. Therefore, regenerated bacterial cellulose fibers prepared by the NMMO·H_2O process could be a new kind of environment friendly cellulose fiber. But more work should be done to improve its mechanical properties of the regenerated BC fibers.

Acknowledgement

This research was financially supported by State Key Laboratory for Modification of Chemical Fibers and Polymer Materials (No. LZ0902).

References

Belousova, T. A., Shablygin, M. V., Belousova, Y. Y., Golova, L. K., & Papkov, S. P. (1986). Spectrum feature of the N-methylmorpholine-N-oxide-water-cellulose system. *Polymer Science*, *28*(5), 1115–1122.
Brown, A. L. (1886). On an acetic ferment which forms cellulose. *Chemical Society*, *49*, 432–439.
Dwianto, W., Norimoto, M., Morooka, T., Tanaka, F., Inoue, M., & Liu, Y. (1998). Radial compression of sugi wood. *Holz Roh Werkst*, *56*, 403–411.
Fink, H. P., Weigel, P., Purz, H. J., & Ganster, J. (2001). Structure formation of regenerated cellulose materials from NMMO-solutions. *Progress in Polymer Science*, *26*, 1473–1524.
Hindeleh, A. M., & Johnson, D. J. (1972). Crystallinity and crystallite size measurement in cellulose fibers: 1. Ramie and fortisan. *Polymer*, *13*, 423–430.
Jonas, R., & Farah, L. F. (1998). Production and application of microbial cellulose. *Polymer Degradation and Stability*, *59*(1), 101–106.
Liang, C. Y., & Marchessault, R. H. (1959). Infrared spectra of crystalline polysaccharides. I Hydrogen bonds in native cellulose. *Polymer Science*, *37*, 385–395.
Liu, R. G., Shao, H. L., & Hu, X. C. (2001). The online measurement of Lyocell fibers and investigaetion of elongational viscosity of cellulose N-methylmorpholine-N-oxide monohydrate solutions. *Macromolecular Materials and Engineering*, *286*, 179–186.
Liu, R. G., Shen, Y. Y., Shao, H. L., Wu, C. X., & Hu, X. C. (2001). An analysis of Lyocell fiber formation as a melt-spinning process. *Cellulose*, *8*, 13–21.
Lock R.L. (1992). Process for spinning polypeptide fiber. US Patent Office, Pat. No. 5 171 505.
Pommet, M., Juntaro, J., Heng, J. Y., Mantalaris, M., Lee, A. F., Wilson, K., et al. (2008). Surface modification of natural fibers using bacteria: depositing bacterial cellulose on to natural fibers to create hierarchical fiber reinforced nanocomposites. *Biomacromolecules*, *9*(6), 1643–1651.
Rosenau, T., Potthast, A., Adorjan, I., Hofinger, A., Sixta, H., Firgo, H., et al. (2002). Cellulose solutions in N-methylmorpholine-N-oxide(NMMO) degradation processes and stabilizers. *Cellulose*, *9*(324), 283–291.
Rosenau, T., Potthast, A., Sixta, H., & Kosma, P. (2001). The chemistry of side reactions and byproduct formation in the system NMMO/cellulose (Lyocell process). *Progress in Polymer Science*, *26*, 1763–1837.
Ross, P., Mayer, R., & Benziman, M. (1991). Cellulose biosynthesis and function in bacteria. *Microbiology and Molecular Biology Reviews*, *55*(1), 35–58.
Smidt, E., Lechner, P., Schwanninger, M., Haberhauer, G., & Gerzabek, M. H. (2002). Characterization of waste organic matter by FT-IR spectroscopy: application in waste science. *Applied Spectroscopy*, *56*(9), 1170–1175.
Svensson, A., Nicklasson, E., Harrah, T., Panilaitis, B., Kaplan, D. L., Brittberg, M., et al. (2005). Bacterial cellulose as a potential scaffold for tissue engineering of cartilage. *Biomaterials*, *26*, 419–431.
Zhang, J. X., Luo, J., Tong, D. M., Zhu, L. F., Dong, L. L., & Hu, C. W. (2010). The dependence of pyrolysis behavior on the crystal state of cellulose. *Carbohydrate Polymers*, *79*(1), 164–169.
Zhu, K. R., Zhang, M. S., Hong, J. M., & Yin, Z. (2005). Size effect on phase transition sequence of TiO2 nanocrystal. *Materials Science and Engineering A*, *403*(2005), 87–93.